THE JOURNAL OF PHYSICAL CHEMISTRY Letters

Letter

pubs.acs.org/JPCL

Velocity Fluctuations in Helical Propulsion: How Small Can a Propeller Be

Arijit Ghosh,[†,#] Debadrita Paria,[§,#] Govindan Rangarajan,[‡] and Ambarish Ghosh*[,†,⊥,§]

[†]Department of Electrical Communication Engineering, [§]Centre for Nano Science and Engineering, [‡]Department of Mathematics, and [⊥]Department of Physics, Indian Institute of Science, Bangalore 560012, India

Supporting Information

ABSTRACT: Helical propulsion is at the heart of locomotion strategies utilized by various natural and artificial swimmers. We used experimental observations and a numerical model to study the various fluctuation mechanisms that determine the performance of an externally driven helical propeller as the size of the helix is reduced. From causality analysis, an overwhelming effect of orientational noise at low length scales is observed, which strongly affects the average velocity and direction of motion of a propeller. For length scales smaller than a few micrometers in aqueous media, the operational frequency for the propulsion system would have to increase as the inverse cube of the size, which can be the limiting factor for a helical propeller to achieve locomotion in the desired direction.

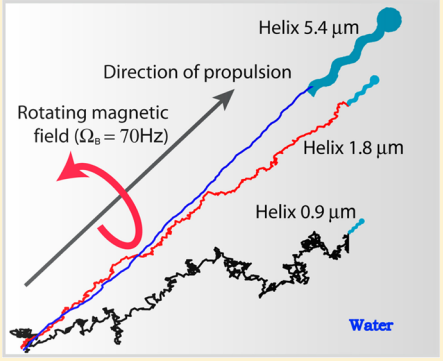

SECTION: Glasses, Colloids, Polymers, and Soft Matter

From large submarines to various flagellated microorganisms, a wide range of natural and artificial swimmers utilize helical propulsion to move in fluidic environments. The essence of the locomotion strategy lies in the coupling of translation and rotation that is possible in a helical shape,[1] which can be powered internally in self-propelled swimmers, such as through internal biochemical mechanisms as in many bacterial species[2] or externally, for example, in a magnetized screw[3] under the action of an externally applied rotating magnetic field. The method of helical propulsion becomes especially important at smaller length scales, where inertial effects are dominated by viscous forces (low Reynolds number), thereby requiring the swimmer to have nonreciprocal strokes[4] in order to achieve locomotion. This is possible in a helical shape by virtue of its inherent chirality; in fact, helical propulsion is one of the few available methods for achieving locomotion when the Reynolds number is significantly less than unity.

At low length scales, the effects of thermal fluctuations become non-negligible, which can give rise to many fascinating features, both in isolation[5,6] as well as through fluidic interactions in a collection[7−10] of internally powered (self-propelled) swimmers. In particular, fluctuations in the orientation of the swimmer can play a strong role, which, for example, can result in ballistic motion at short time scales and diffusive motion at time scales much larger than the orientation diffusion. This is one important aspect where self-propelled swimmers differ from externally driven (helical) propellers because unlike a self-propelled swimmer, the motion of a propeller is always tied to the characteristics of the external power source, resulting in a direction of motion completely determined by the external drive. The central question addressed in this Letter is how thermal noise affects the motion of an externally driven helical propeller, in particular, the origin of speed fluctuations of a driven system and the deviation of the propeller from the path set by the external drive.

A detailed study of velocity fluctuations in helical propulsion can improve our understanding of the role of thermal noise in the motion of swimmers under external stimuli, for example, that of certain species of bacteria under chemical[11] gradients. Besides serving as model artificial systems to understand the locomotion of living matter, fascinating biomedical applications have been envisioned[12−14] and demonstrated[15,16] with artificial propellers in recent years. Specifically important are magnetic propellers[17,18] that have been actuated and maneuvered with small rotating magnetic fields in various biological fluids and have been predicted to be useful in drug delivery,[19,20] intra- and extracellular microrheological measurements, microsurgery, and many other important biomedical applications.[21] In all of these applications, the role of thermal fluctuations can cause the propeller to deviate from the intended path, thus limiting the accuracy and thereby the functionality of this system.

A quantity commonly used to estimate the effect of thermal noise on driven systems is the Peclet number, which is defined as the ratio of the advective to the diffusive transport rate of particles in a suspension. While *Pe* (Peclet number) can provide meaningful insight on the relative importance of thermal noise in any type of driven motion, the case of a rotating, and

Received: October 10, 2013
Accepted: December 2, 2013
Published: December 2, 2013

   dx.doi.org/10.1021/jz402186w | *J. Phys. Chem. Lett.* 2014, 5, 62−68

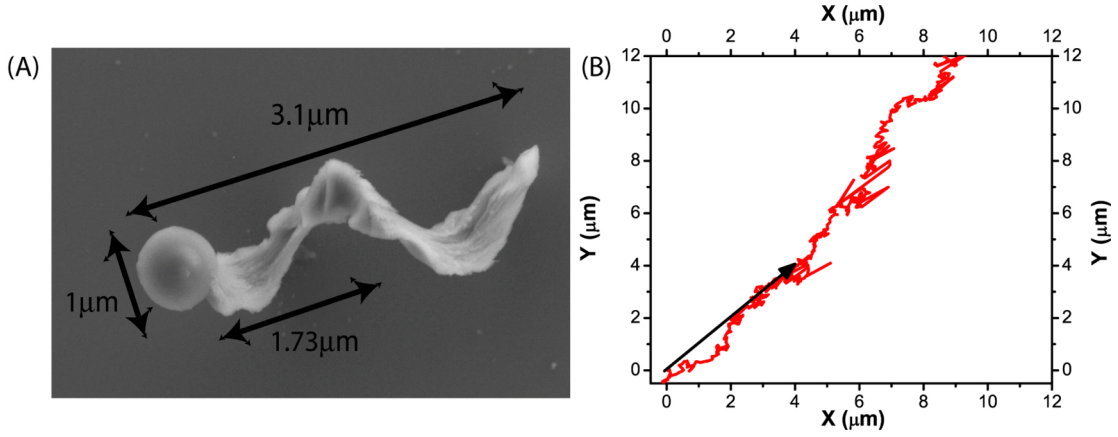

Figure 1. (A) SEM image of a typical propeller used in the experiments. (B) Typical trajectory of the propeller taken for 10 s under the action of a magnetic field rotating at 15 Hz. The intended direction of motion is depicted by the arrow.

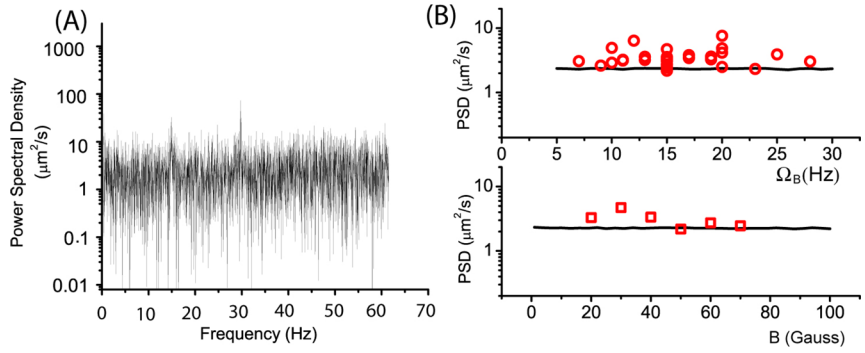

Figure 2. (A) Typical PSD of the velocity of propulsion. The images were obtained at 120 frames per second. (B) Experimental PSD as a function of magnetic field frequency, Ω_B (circles) and magnetic field strength, B (squares), along with numerical estimates (solid lines).

therefore translating helix, needs to be dealt with caution. This is due to the presence of multiple degrees of freedom, which can cause the helical structure to undergo translational and rotational diffusion[22] along and about various symmetry axes, which in turn raises the question regarding which particular diffusion is of highest importance.[23] This has been elaborated on in greater detail later in this Letter. Apart from *Pe*, we have also considered a quantity termed as "directionality",[24] which provides a quantitative estimate of the deviation of the propeller from its intended path. This is defined as $\chi = L_p/S$, where L_p is the displacement of the propeller in the intended direction of propulsion and S is the sum of the displacements traveled by the propeller. Note that S is different from purely diffusive root-mean-square displacement but rather refers to the sum of the absolute values of the displacements. We checked with numerical simulations that the quantity χ was independent of the time of measurement.

The aim of this Letter is to measure and understand the velocity fluctuations of an externally driven helical propulsion system and analyze the underlying mechanisms causing these fluctuations. In particular, we have analyzed the effect of the size of the propeller on the directionality of motion and investigated whether there is a strict limitation of size below which helical propulsion will be impossible to achieve. These studies, different from the size limit studies for free swimmers,[25] are necessary for efficient design,[26] as well as to find the limitations of an existing propulsion system.

The experimental system, in particular, the methods of fabrication and actuation, have been discussed in detail before.[17,27,28] In essence, a helical nanostructure (SEM image shown in Figure 1A) made of SiO_2 was fabricated on a monolayer of polystyrene beads using a physical vapor deposition method called glancing angle deposition (GLAD),[29] subsequently coated with a ferromagnetic material (cobalt) with electron beam evaporation. We magnetized the structures such that the applied fields were perpendicular to the long axis of the propellers, which ensured that the magnetic moments were perpendicular to the long axis. A very dilute solution of the propellers was dispersed in DI water, from where a small drop (~7−8 μL) was placed between two coverslips. The solution was made very dilute to ensure that the propellers do not aggregate and are far separated so as to not have any magnetic interactions. After sealing the coverslips, the solution was found to wet approximately 1.5 × 1.5 cm^2 of the glass surfaces, implying the fluidic chamber to be approximately 30−35 μm thick. The propellers were actuated by applying a rotating magnetic field of strength B and frequency Ω_B in a triaxial Helmholtz coil mounted on an optical microscope, which was captured with a CMOS camera at a frame rate at least 4 times higher than the driving frequency Ω_B. The motion of the propeller was tracked with an image processing code, where the image of the propeller in each frame was fitted to an ellipsoidal shape. The centroid and orientation of the ellipse provided the position and orientation of the propeller in each frame. A typical trajectory of the propeller is shown in Figure 1B.

An important quantity of interest obtained from the trajectory was the velocity v_p in the intended direction of propulsion and its power spectral density (PSD). A typical PSD is shown in Figure 2A,

dx.doi.org/10.1021/jz402186w | J. Phys. Chem. Lett. 2014, 5, 62−68

which was found to be flat across the frequency spectrum, implying the sources of velocity fluctuations to have a Gaussian probability distribution, as is normally the case in simple fluids like DI water. It should be noted that the time scale of our experimental study was limited by the maximum frame rate; it is not possible to comment whether there are non-Gaussian fluctuation effects present at other time scales. For example, the momentum relaxation time of the propellers, given by the ratio of the mass to the friction coefficients, is extremely short ($\sim 10^{-7}$ s). The magnitude of the PSD was found to be independent of the strength (B) and frequency (Ω_B) of the rotating magnetic field and was reasonably close to the results obtained from the numerical simulations, described below.

Numerical Simulations. We assumed the propeller to be a rigid body in bulk, far from any surface or any other interacting propeller, in the numerical simulations. The calculations required the construction of the 6 × 6 friction coefficient tensor

$$[\Gamma] = \begin{bmatrix} \Gamma_T & \Gamma_C \\ \Gamma_C^t & \Gamma_R \end{bmatrix}$$

where Γ_T, Γ_R, and Γ_C (and its transpose) are second-order tensors, denoting the translational, rotational, and coupling terms of the friction, respectively. These quantities were mostly derived from various experimentally measured diffusion constants as follows. The propeller undergoing Brownian motion was imaged over a long time. From the video data obtained, the mean-square displacements in the body frame along the major and minor axes as well as the rotational mean-square displacement about the short axis were obtained. The slopes of the MSD curves for the first few data points give the values of the corresponding diffusion coefficients using the relation $x^2(t) = 2Dt$. The two translational diffusion coefficients, along the long and short axes, were measured experimentally (body frame measurements) from the slope of the mean-square displacement curves using the relation $\langle(\Delta x(t))^2\rangle = 2D_T t$. Their values were measured to be $D_{t3} = 0.585\ \mu m^2/s$ and $D_{t1} = 0.563\ \mu m^2/s$, respectively. Also, the rotational diffusion coefficient about the short axis could be measured using $\langle(\Delta\theta(t))^2\rangle = 2D_{r1}t$ and was found to be $D_{r1} = 0.2498\ rad^2/s$. The theoretical values for a helical flagellum of similar dimensions are 0.131 $\mu m^2/s$, 0.103 $\mu m^2/s$, and 0.21 rad^2/s, respectively, as estimated using ref 1. The difference between the experimental and the theoretical estimates of the diffusion constants was probably due to the assumption of a thin flagellum in the theoretical estimate, while the helices used in our experiments were significantly thicker. We estimated the rotational friction coefficient about the long axis to be $\Gamma_{r3} \approx 10^{-21}$ SI units using formulas from ref 1. Because no net force was exerted by the external magnetic field, we obtain from the linearity of Stokes flow $v_p/\Omega_B = -\Gamma_{c3}/\Gamma_{t3}$. This ratio refers to a condition where thermal fluctuations are negligible. Accordingly, we measured this ratio at the highest possible magnetic field frequencies (Ω_B), where the estimated directionality ($\chi = L_p/S$, as defined before) of motion was almost 1, implying negligible effects of thermal noise. This ratio is referred to as the no-noise pitch (p_0) and was measured to be around 380 nm.

The inverse relationship between the diffusion coefficient D and the friction coefficient tensors[30] is represented by $[D] = kT[\Gamma]^{-1}$, which provides $D_{t3} = kT[\Gamma_{r3}/(\Gamma_{t3}\Gamma_{r3} - \Gamma_{r3}^2)]$, where D_{t3} is the translational diffusion along the long axis. Γ_{t3}, Γ_{r3}, and Γ_{c3} are the translational, rotational, and coupling drags along the long axis. Using the equation for the no-noise pitch and the above relation between drag and diffusion, we can solve for the translational drag Γ_{t3} and the coupling drag Γ_{c3}. The coupling friction coefficient terms along the other axes were 0. Hence, the other drag coefficients Γ_{t1}, Γ_{t2}, Γ_{r1}, and Γ_{r2} can be found simply by using $\Gamma_{t1} = \Gamma_{t2} = kT/D_{t1}$ and $\Gamma_{r1} = \Gamma_{r2} = kT/D_{r1}$, thereby providing all of the terms to describe the friction tensor Γ.

The external rotating magnetic field exerts a torque given by $\vec{\tau} = \vec{m} \times \vec{B}$, a three element vector, where $\vec{m}$ and $\vec{B}$ denote the permanent magnetic moment of the propeller and the magnetic field, respectively. The value of the magnetic moment is estimated from the step out frequency of the propeller, the frequency at which the propeller could not rotate in sync with the rotating magnetic field, given by $\Omega_{step} = mB/2\pi\Gamma_{r3}$, for a propeller having the moment along the short axis.[27,28] For a magnetic field value of ~5 mT and $\Omega_{step} \approx 50$ Hz, we obtain the value of the moment, $m \approx 10^{-16}$ A m^2. To include the effect of thermal noise, we used the method described in ref 31 and introduced the random force term F_R, described by a Gaussian distribution with zero mean and the variance, given by $\langle F_R(t) F_R'(t')\rangle = 2kT\Gamma\delta(t - t')$. The smallest time step Δt used in the simulation is taken to be much smaller than the lowest time scale in the system, which is $\tau_{r3} = 1/(2D_{r3})$, approximately equal to 0.08 s for the propellers used in these experiments. The external force and torque can be written as

$$F_{ext} = \begin{bmatrix} 0 \\ \vec{\tau} \end{bmatrix}$$

We have ignored inertial effects in all of our simulations as the Reynolds number under consideration is very small ($\sim 10^{-5}$). Accordingly, we solve for the velocity vector (translational and rotational) given by $v = \Gamma^{-1}(F_{ext} + F_R)$, where v provides the instantaneous linear and angular velocities of the propeller, from where the time evolution of the propeller coordinates in the body frame could be obtained. To transform these coordinates between lab and body frames, we used the transformation matrix **R**, defined in terms of the Euler parameters (quaternions).

A key parameter relevant to this study was the magnitude of the external torque $\vec{\tau} = \vec{m} \times \vec{B}$, where $\vec{m}$ and $\vec{B}$ refer to the magnetic moment of the propeller and strength of the applied field, respectively. For the experiments and numerical simulations presented here, the magnitude of the applied torque $|\vec{\tau}|$ was chosen to be significantly larger than the thermal energy k_BT, such that the magnetic moment always remained aligned by the external field. In other words, we assumed the available power from the source to be infinite and neglected fluctuations that could arise due to the misalignment of the moment with respect to the magnetic field, which was valid in our experimental system. Under this condition, the PSD remained independent of the frequency and strength of the magnetic field, as seen in the results shown in Figure 2B.

Effect of Proximity to a Surface. While the calculations assumed the propeller to be completely isolated, it was not possible to ensure that the propeller did not come close to the chamber walls during the experimental measurements. To investigate if the velocity fluctuations were indeed affected by the presence of a surface in close proximity, we placed the propellers in fluidic chambers that were significantly thinner than the ones described before. This was achieved by placing a small drop (~0.4−0.5 μL) of propeller suspension between two thoroughly cleaned (Piranha cleaning) coverslips. After sealing

dx.doi.org/10.1021/jz402186w | J. Phys. Chem. Lett. 2014, 5, 62−68

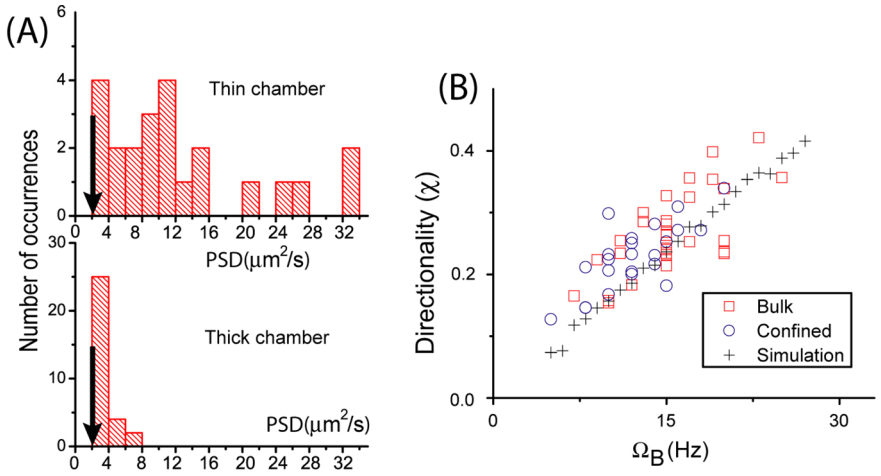

Figure 3. (A) Histograms of experimentally measured PSD in thin and thick chambers. The arrows indicate the average PSD value (2.9 $\mu m^2/s$) obtained from numerical calculation considering bulk behavior. (B) The calculated and measured (both thin and thick chambers) directionality as a function of magnetic field frequency.

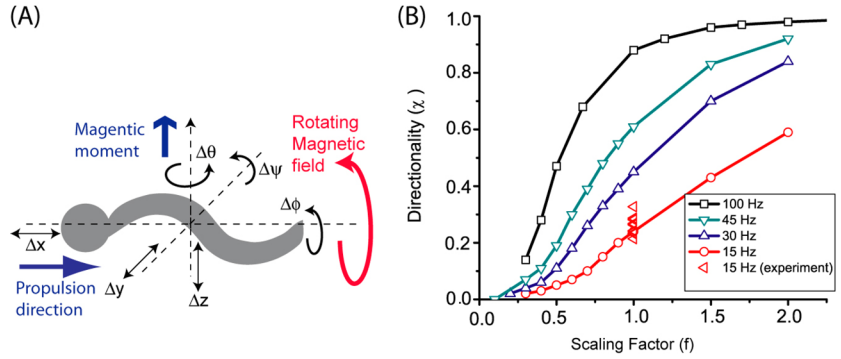

Figure 4. (A) Schematic of various fluctuation mechanisms affecting the motion of the propeller. The angular coordinates given as θ, ϕ, and ψ should not be confused with the Euler angles. (B) Directionality as a function of the size scaling factor, for both numerical and experimental data at various magnetic field frequencies, Ω_B. The scaling factor in the dimensions was with respect to the propeller shown in Figure 1A.

the coverslips, the solution was found to wet approximately 1×1 cm^2 of the glass surfaces, implying the fluidic chamber to be approximately 3−5 μm thick.

In Figure 3A, we show mean values of the PSD of the propulsion velocities measured in thick and thin chambers, along with the numerical estimate denoted by an arrow, obtained assuming no surface interaction. It is evident that the noise level as well as the variability of the noise level (spread in the histograms) was significantly higher[31] in the thinner chambers, which was most probably due to enhanced interactions of the propeller with the surface of the chamber. Though the experiments in thick chambers were intended to eliminate the effect of surface, it was not always the case as there was no direct control on the distance between the bottom surface and the propeller. This resulted in some variability in the PSD in the thicker chambers as well; however, the lower values of the experimentally obtained PSD in the thicker chambers indeed corresponded to the bulk theoretical estimate.

Apart from an increase in the average noise level under confinement, the velocity power spectra for propellers under confinement were not perfectly flat and sometimes showed peaks at the multiples of the driving frequency Ω_B. Understanding these effects will probably require a detailed numerical simulation, which is beyond the scope of the present Letter and will be discussed in a future publication. The main point to note is the increase in the overall velocity noise in confined geometries, which is almost definitely related to the interaction of the propeller with the adjacent surface(s). It is known that certain types of self-propelled swimmers (pushers)[32] are likely to be found near the wall due to hydrodynamic attraction to the surfaces. At such small distances from the wall, they experience a torque[33] that causes them to be parallel to the wall, through the formation of image force dipoles. In the present case, the propeller may become nonparallel to the wall due to orientational fluctuations, thus resulting in a restoring torque arising from hydrodynamic interactions with the chamber walls. The effect of the restoring torque is expected to be more in confined geometries. Surprisingly, though the mean PSD was found to be higher in thin chambers, the directionality remained independent of confinement and matched well with the numerical calculations, as shown in Figure 3B, where the directionality is plotted as a function of Ω_B for experiments conducted in both thin and thick chambers.

Microscopic Origin of Velocity Fluctuations: Size Limit of Helical Propulsion. As discussed in the prior sections, the numerical simulations and the bulk experiments (thicker chambers) were in overall agreement, implying the general validity of the theoretical model used here. However, numerical simulations could not provide a microscopic understanding of the origin of fluctuations in this system, which we try to address in the present section.

dx.doi.org/10.1021/jz402186w | J. Phys. Chem. Lett. 2014, 5, 62−68

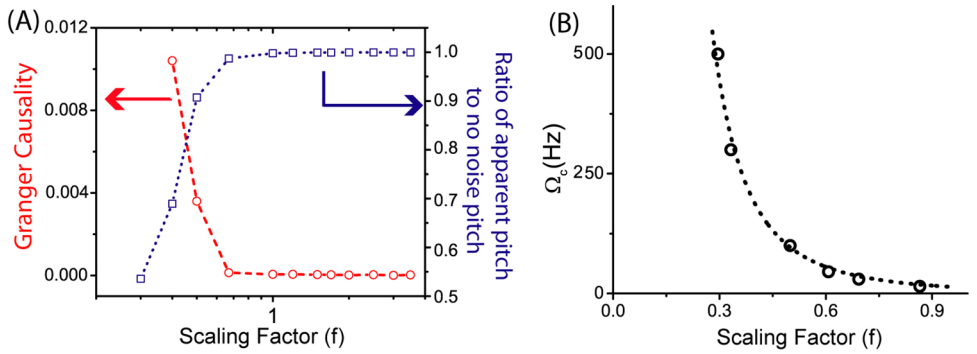

Figure 5. (Left) Granger causality from $\cos^2(\theta)$ to v_p and (right) ratio of apparent to no-noise pitch as a function of the scaling factor for Ω_B = 100 Hz. (D) Frequency Ω_c at which $p_a = 0.9\ p_0$ as a function of the scaling factor; the dotted line shows the f^{-3} dependence.

Schematics of the different linear and angular displacements in the body frame of the propeller are shown in Figure 4A, which could originate from thermal noise. Of these possibilities, angular displacements $\Delta\phi$ and $\Delta\psi$, as shown in the figure, varied as $\exp(-\vec{m}\cdot\vec{B}/k_BT)$ and therefore were vanishingly small for the conditions assumed in this Letter. Much more interesting are the translational displacement along the short axes (Δy and Δz) and the rotational fluctuation about the short axis ($\Delta\theta$), all of which could occur while having the moment aligned to the field and therefore remained independent of the strength of the applied torque. More subtle was the translation along the long axis (Δx), which could be accompanied by a small rotation about the long axis ($\Delta\phi$) by virtue of the translation−rotation coupling term (Γ_c). To understand how the various degrees of freedom affected the velocity fluctuations, we considered the directionality χ of a driven propeller of the same geometrical characteristics, as shown in Figure 1A, and investigated the variation of directionality when all of the propeller dimensions were scaled by a factor f. This implied a scaling of the friction coefficient tensor, approximately given by

$$\begin{bmatrix} \Gamma_T & \Gamma_C \\ \Gamma_C & \Gamma_R \end{bmatrix} \rightarrow \begin{bmatrix} f\Gamma_T & f^2\Gamma_C \\ f^2\Gamma_C & f^3\Gamma_R \end{bmatrix}$$

The numerical along with the experimental results for f = 1 are shown in Figure 4B. For a fixed length scale, χ increased with Ω_B, which is expected because v_p changed linearly with Ω_B while the fluctuations remained independent of the frequency. The most interesting observation was the reduction of χ to almost zero at around f = 0.3 for the frequencies shown here, which points toward the possible existence of a length scale below which it is not possible to have driven helical propulsion. It is important to note that the scaling of the friction tensor does not depend on the finer details of the helical geometry, such as the attached microbead. Also, as observed from the SEM images, the surface of the propeller has significant roughness, which depends on the details of fabrication and thus may be independent of the scaling factor. It is not known from existing literature how the surface roughness may affect the friction tensor.

The loss of directionality at lower length scales is obviously due to contributions of the various fluctuations mechanisms to the velocity noise; however, it is not clear which particular degree of freedom of fluctuation would be the leading cause behind the propulsion mechanism. From physical arguments, we expect the diffusion of the rotation angle (θ) about the short axis, which varies as f^{-3}, to dominate over the translational diffusivities, which scale as f^{-1}, but it is not clear at which length scale the fluctuations in θ indeed become the dominating factor determining the motion of the propeller. To estimate the causal relation of the velocity noise with the various fluctuation mechanisms, we have used a technique called Granger Causality,[34] which has become the leading statistical technique for determining causal relations between processes in recent times. We use this method instead of cross-correlation because Granger Causality (more details in the Supporting Information) specifically incorporates the flow of time in its definition, whereas cross-correlation does not do so.

As shown in Figure 5A, we have estimated the degree of causal influence from $\cos^2(\theta)$ to v_p as a function of the scaling factor f, which was obtained by analyzing the time series of θ and v_p. A dramatic rise of the causality is clearly seen below a particular length scale, whose exact value depended on Ω_B. A closely related quantity was the apparent pitch of the propeller, given by $p_a = v_p/\Omega_B$, and how it varied with the scaling factor f. In the presence of Gaussian translational noise only, v_p and therefore p_a were expected to be unchanged from the no-noise value of the pitch (p_0). The same would be expected for Gaussian angular fluctuations about the long axis. The role of θ_N was much more subtle, in which any fluctuation in the orientation of the propeller resulted in a misalignment from the direction of propulsion, which could only reduce the average propulsion velocity and therefore the apparent pitch. The ratio of the apparent to the no-noise pitch (p_a/p_0) as a function of the scaling factor is plotted in Figure 5A for Ω_B = 100 Hz. The results indicate a sudden reduction in the apparent pitch below a particular length scale, which matched very well with the point at which the causal influence of θ_N to v_p increased.

It is interesting to note that the smallest artificial helical propeller made to date[17] is about 1.5 μm long, reasonably close to the limits obtained here. Accordingly, it is natural to ask if the large reduction of the apparent pitch and the directionality around f = 0.3 (implying length ≈ 1 μm) will occur even if the geometry of the propeller, such as the width and pitch of the helix, or the experimental parameters, such as B and frequency Ω_B, are different. In the simplest approximation, the helical shape can be approximated as an ellipsoid, in which θ_N varies as L^{-3}; here, L is the length of the ellipsoid.[35] Ignoring the weak logarithmic terms that depend on the aspect ratio of the ellipsoid, L is the dominating factor that determines the propeller fluctuation dynamics for small lengths with little or no influence from other geometrical parameters such as the pitch or the width. The strength of the magnetic torque $|\vec{\tau}|$, would

dx.doi.org/10.1021/jz402186w | J. Phys. Chem. Lett. 2014, 5, 62−68

play little role as long as the strength is large enough for the propeller to be rotated in sync with the magnetic field. Increasing Ω_B would increase the apparent pitch simply because of the greater distance traveled by the propeller within the time in which orientational misalignment would occur. In other words, the time scale of the rotating field, given by $1/\Omega_B$, needs to be shorter than the time scale of θ diffusion τ_θ, which in turn varies as L^3, assuming an ellipsoidal geometry of length L and ignoring the weak logarithmic terms. Note that the ratio $(1/\Omega_B)/\tau_\theta$ can be interpreted as the Peclet number, defined here as the advective (here rotation about the long axis) to the diffusive (angular diffusion about the short axis) time scales. To obtain a firm quantitative prediction, we estimated that the frequency Ω_c at which $p_a = 0.9p_0$, which as shown in Figure 5B, indeed increased as a function of L^{-3}. To summarize these observations, even in the presence of an infinitely large available torque that can be obtained from choosing the right materials or powerful driving electronics, the minimum size for a useful helical propeller is finally limited by orientational fluctuations, which can be the dominating factor at small sizes. To obtain any useful motion (nonzero directionality), the maximum available frequency of the magnetic field needs to increase as the inverse cube of the size of the propeller, which could be a limiting factor under practical experimental conditions. It will be interesting to see if similar effects of shape can also arise in chemically powered systems as well.[36]

In conclusion, we have measured and studied the origin of velocity fluctuations in driven helical propulsion and observed an overwhelming effect of orientational thermal noise at small length scales. Assuming a propulsion system that can supply infinite torque and rotation frequency, a propeller can be made arbitrarily small. However, at length scales smaller than a few micrometers, the operational frequency for such systems would have to increase as L^{-3}, which can be a limiting factor for a helical propeller to achieve locomotion in the desired direction. Considering practical limitations, such as a possible dependence of the magnetic moment on the volume ($\sim L^3$) of the propeller, the step out frequency (defined as the magnetic field frequency at which the maximum available torque is equal to the viscous drag) will also scale as L^3. Accordingly, one would have to increase the magnetic field by the same amount to ensure that the propeller would rotate synchronously with the rotating field. This would imply the operational frequency to be an even stronger function of the size, which may pose a serious obstacle to various promising nanoscale applications envisioned with "nano"-propellers. The present study was done in aqueous environments at room temperature; it is easy to see that the size limitation will be decreased if more viscous fluids or lower temperatures are assumed. The analysis can be easily extended to nonmagnetic systems, for example, in the application of a rotating rf electric field to a racemic mixture of dipolar chiral molecules in order to extract a single enantiomer,[37] a scheme[38] subject to similar limitations arising from orientational fluctuations.

■ ASSOCIATED CONTENT

Supporting Information

Discussion of the Granger Causality. This material is available free of charge via the Internet at http://pubs.acs.org.

■ AUTHOR INFORMATION

Corresponding Author

*E-mail: ambarish@ece.iisc.ernet.in.

Author Contributions

#A. Ghosh and D. Paria contributed equally.

Notes

The authors declare no competing financial interest.

■ ACKNOWLEDGMENTS

The authors thank Prabhu Nott for helpful discussions and the Department of Biotechnology (DBT) for funding this work, and they gratefully acknowledge the use of the facilities in Micro and Nano Characterization Facility (MNCF, CeNSE) at IISc. This work is partially supported by the Ministry of Communication and Information Technology under a grant for the Centre of Excellence in Nanoelectronics, phase II. G.R. was supported by the JC Bose Fellowship, DST Centre for Mathematical Biology and UGC Centre for Advanced Study. G.R. is an Honorary Professor at the Jawaharlal Nehru Centre for Advanced Scientific Research, Bangalore.

■ REFERENCES

(1) Lighthill, J. Flagellar Hydrodynamics. *SIAM Rev.* **1976**, *18*, 161−230.
(2) Berg, H. C.; Anderson, R. A. Bacteria Swim by Rotating Their Flagellar Filaments. *Nature* **1973**, *245*, 380−382.
(3) Ishiyama, K.; Sendoh, M.; Yamazaki, A.; Arai, K. I. Swimming Micro-machine Driven by Magnetic Torque. *Sens. Actuators, A* **2001**, *91*, 141−144.
(4) Purcell, E. M. Life at Low Reynolds Number. *Am. J. Phys.* **1977**, *45*, 3−11.
(5) Dunkel, J. R.; Zaid, I. M. Noisy Swimming at Low Reynolds Numbers. *Phys. Rev. E* **2009**, *80*, 021903.
(6) Garcia, M. L.; Garcia, M.; Berti, S.; Peyla, P.; Rafaï, S. Random Walk of a Swimmer in a Low-Reynolds-Number Medium. *Phys. Rev. E* **2011**, *83*, 035301.
(7) Chen, D. T. N.; Lau, A. W. C.; Hough, L. A.; Islam, M. F.; Goulian, M.; Lubensky, T. C.; Yodh, A. G. Fluctuations and Rheology in Active Bacterial Suspensions. *Phys. Rev. Lett.* **2007**, *99*, 148302.
(8) Simha, R. A.; Ramaswamy, S. Hydrodynamic Fluctuations and Instabilities in Ordered Suspensions of Self-Propelled Particles. *Phys. Rev. Lett.* **2002**, *89*, 058101/1−058101/4.
(9) Sokolov, A.; Apodaca, M. M.; Grzybowski, B. A.; Aranson, I. S. Swimming Bacteria Power Microscopic Gears. *Proc. Natl. Acad. Sci. U.S.A.* **2010**, *107*, 969−974.
(10) Wu, X.-L.; Libchaber, A. Particle Diffusion in a Quasi-Two-Dimensional Bacterial Bath. *Phys. Rev. Lett.* **2000**, *84*, 3017−3020.
(11) Xie, L.; Altindal, T.; Chattopadhyay, S.; Wu, X. L. Bacterial Flagellum as a Propeller and as a Rudder for Efficient Chemotaxis. *Proc. Natl. Acad. Sci. U.S.A.* **2011**, *108*, 2246−2251.
(12) Ebbens, S. J.; Howse, J. R. In Pursuit of Propulsion at the Nanoscale. *Soft Matter* **2010**, *6*, 726−738.
(13) Fischer, P.; Ghosh, A. Magnetically Actuated Propulsion at Low Reynolds Numbers: Towards Nanoscale Control. *Nanoscale* **2011**, *3*, 557−563.
(14) Wang, J.; Manesh, K. M. Motion Control at the Nanoscale. *Small* **2010**, *6*, 338−345.
(15) Tottori, S.; Zhang, L.; Qiu, F.; Krawczyk, K. K.; Obregón, A. F.; Nelson, B. J. Magnetic Helical Micromachines: Fabrication, Controlled Swimming, and Cargo Transport. *Adv. Mater.* **2010**, *24*, 811−816.
(16) Xi, W.; Solovev, A. A.; Ananth, A. N.; Gracias, D. H.; Sanchez, S.; Schmidt, O. G. Rolled-up Magnetic Microdrillers: Towards Remotely Controlled Minimally Invasive Surgery. *Nanoscale* **2013**, *5*, 1294−1297.
(17) Ghosh, A.; Fischer, P. Controlled Propulsion of Artificial Magnetic Nanostructured Propellers. *Nano Lett.* **2009**, *9*, 2243−2245.
(18) Zhang, L.; Abbott, J. J.; Dong, L.; Kratochvil, B. E.; Bell, D.; Nelson, B. J. Artificial Bacterial Flagella: Fabrication and Magnetic Control. *Appl. Phys. Lett.* **2009**, *94*, 064107/1−064107/3.

(19) Cotí, K. K.; Belowich, M. E.; Liong, M.; Ambrogio, M. W.; Lau, Y. A.; Khatib, H. A.; Zink, J. I; Khashab, N. M.; Stoddart, J. F. Mechanised Nanoparticles for Drug Delivery. *Nanoscale* **2009**, *1*, 16−39.
(20) Dogangil, G. R.; Ergeneman, O.; Abbott, J. J.; Pane, S.; Hall, H.; Muntwyler, S.; Nelson, B. J. *Toward Targeted Retinal Drug Delivery with Wireless Magnetic Microrobots*. 2008 IEEE/RSJ International Conference on Intelligent Robots and Systems, Nice, France, Sept 22−26, 2008; pp 1921−1926.
(21) Nelson, B. J.; Kaliakatsos, I. K.; Abbott, J. J. Microrobots for Minimally Invasive Medicine. *Annu. Rev. Biomed. Eng.* **2010**, *12*, 55−85.
(22) Butenko, A. V.; Mogilko, E.; Amitai, L.; Pokroy, B.; Sloutskin, E. Coiled to Diffuse: Brownian Motion of a Helical Bacterium. *Langmuir* **2012**, *28*, 12941−12947.
(23) Dunderdale, G.; Ebbens, S.; Fairclough, P.; Howse, J. Importance of Particle Tracking and Calculating the Mean-Squared Displacement in Distinguishing Nanopropulsion from Other Processes. *Langmuir* **2012**, *28*, 10997−11006.
(24) Sahari, A.; Headen, D.; Behkam, B. Effect of Body Shape on the Motile Behavior of Bacteria-Powered Swimming Microrobots (BacteriaBots). *Biomed. Microdevices* **2012**, *14*, 999−1007.
(25) Dusenbery, D. B. Minimum Size Limit for Useful Locomotion by Free-Swimming Microbes. *Proc. Natl. Acad. Sci. U.S.A.* **1997**, *94*, 10949−10954.
(26) Keaveny, E. E.; Walker, S. W.; Shelley, M. J. Optimization of Chiral Structures for Microscale Propulsion. *Nano Lett.* **2013**, *13*, 531−537.
(27) Ghosh, A.; Mandal, P.; Karmakar, S.; Ghosh, A. Analytical Theory and Stability Analysis of an Elongated Nanoscale Object under External Torque. *Phys. Chem. Chem. Phys.* **2013**, *15*, 10817−10823.
(28) Ghosh, A.; Paria, D.; Singh, H. J.; Venugopalan, P. L.; Ghosh, A. Dynamical Configurations and Bistability of Helical Nanostructures Under External Torque. *Phys. Rev. E* **2012**, *86*, 031401.
(29) Hawkeye, M. M.; Brett, M. J. Glancing Angle Deposition: Fabrication, Properties, and Applications of Micro- and Nanostructured Thin Films. *J. Vac. Sci. Technol., A* **2007**, *25*, 1317−1335.
(30) Brenner, H. Coupling Between the Translational and Rotational Brownian Motions of Rigid Particles of Arbitrary Shape: II. General Theory. *J. Colloid Interface Sci.* **1967**, *23*, 407−436.
(31) Sun, X.; Lin, T.; Gezelter, J. D. Langevin Dynamics for Rigid Bodies of Arbitrary Shape. *J. Chem. Phys.* **2008**, *128*, 234107/1−234107/14.
(32) Marx, K. *Self-Propelled Rod-Like Swimmers near Surfaces*. Dissertation. University of Cologne, Germany, 2011.
(33) Berke, A. P.; Turner, L.; Berg, H. C.; Lauga, E. Hydrodynamic Attraction of Swimming Microorganisms by Surfaces. *Phys. Rev. Lett.* **2008**, *101*, 038102.
(34) Granger, C. W. J. Investigating Causal Relations by Econometric Models and Cross-Spectral Methods. *Econometrica: Journal of the Econometric Society* **1969**, 424−438.
(35) Perrin, F. Mouvement Brownien d'un Ellipsoide (II). Rotation Libre et Dépolarisation des Fluorescences. Translation et Diffusion de Molécules Ellipsoidales. *J. Phys. Radium* **1936**, *7*, 1−11.
(36) Lugli, F.; Brini, E.; Zerbetto, F. Shape Governs the Motion of Chemically Propelled Janus Swimmers. *J. Phys. Chem. C* **2011**, *116*, 592−598.
(37) Baranova, N. B.; Zel'Dovich, B. Y. Separation of Mirror Isomeric Molecules by Radio-Frequency Electric Field of Rotating Polarization. *Chem. Phys. Lett.* **1978**, *57*, 435−437.
(38) Schamel, D.; Pfeifer, M.; Gibbs, J. G.; Miksch, B.; Mark, A. G.; Fischer, P. Chiral Colloidal Molecules And Observation of The Propeller Effect. *J. Am. Chem. Soc.* **2013**, *135*, 12353−12359.